Fakhari *et al. Robomech J* (2019) 6:15
https://doi.org/10.1186/s40648-019-0143-0

ROBOMECH Journal

RESEARCH ARTICLE Open Access

Modeling and control of planar slippage in object manipulation using robotic soft fingers

Amin Fakhari[1*], Imin Kao[2] and Mehdi Keshmiri[3]

Abstract

Slippage occurrence has an important roll in stable and robust object grasping and manipulation. However, in majority of prior research on soft finger manipulation, presence of the slippage between fingers and objects has been ignored. In this paper which is a continuation of our prior work, a revised and more general method for dynamic modeling of planar slippage is presented using the concept of friction limit surface. Friction limit surface is utilized to relate contact sliding motions to contact frictional force and moment in a planar contact. In this method, different states of planar contact are replaced with a second-order differential equation. As an example of the proposed method application, dynamic modeling and slippage analysis of object manipulation on a horizontal plane using a three-link soft finger is studied. Then, a controller is designed to reduce and remove the undesired slippage which occurs between the soft finger and object and simultaneously move the object on a predefined desired path. Numerical simulations reveal the acceptable performance of the proposed method and the designed controller.

Keywords: Soft finger, Slippage modeling, Friction limit surface, Grasping and manipulation, Slippage control

Introduction

Human hands are one of the most elaborate organs of the human body from dexterity point of view. They can explore, grasp, and manipulate objects of different shapes and materials. Thus, study on design and development of anthropomorphic and dexterous robotic hands is one of the interesting subjects for research.

Contact modeling is the preliminary step in analysis of object grasping and manipulation. Generally, there are two kinds of contact models; point contact and planar contact. When contact is assumed to be a point or deformation in the contact is negligible, this model can be used. The majority of prior research on grasping and manipulation are based on point contact assumption. Coulomb model is usually used for modeling frictional force in the point contact model. For an extensive literature review on grasping and manipulation analysis based on point contact assumption refer to [1]. However, when the contact area is relatively large or deformation in the contact is significant, e.g., soft contact, the point contact model is not applicable. In planar contact, a frictional moment is exerted at the contact interface along with the normal force and tangential frictional force (Fig. 1). This causes a fewer number of contact interfaces to robustly and stably grasp and manipulate an object using soft fingers compared with rigid fingers. Furthermore, the soft fingertips can conform to the objects' uneven surfaces and also damp shocks and vibrations to enhance the stability and robustness of grasp. In the planar contact model, *friction limit surface* is used to relate contact sliding motions to contact frictional force and moment. Goyal et al. [2] first defined the friction limit surface for slippage of a rigid object on a planar surface. Howe and Cutkosky [3] developed a relationship between forces and motions in sliding manipulation. They approximated the friction limit surface to an ellipsoid to simplify control, planning, and simulation of manipulation.

Studies on the robotic hands with soft fingers can be considered in three major groups; soft finger design, soft contact modeling, and soft finger manipulation. The first research group is focused on designing optimized soft fingers [4] and also proper tactile sensors [5]. The second group includes research that focuses on developing

*Correspondence: amin.fakhari@sunykorea.ac.kr; amin.fakhari@outlook.com
[1] Department of Mechanical Engineering, State University of New York, Korea (SUNY Korea), Incheon 21985, Korea
Full list of author information is available at the end of the article

Fig. 1 Normal force, frictional tangential force, and frictional moment in the contact interface of human soft finger

a mathematical model for soft contact. Some of the most important soft contact models are presented in [6–15]. The third group consists of the research focuses on object grasping and manipulation using soft robotic fingers. Arimoto et al. [7, 16] studied grasping and manipulation of a rigid object using soft fingers. To model the softness of fingertips, they assumed a continuous distribution of linear springs located radially within the hemispherical soft fingertip. Kim [8] considered the motion analysis of rigid object manipulation using a pair of soft fingers assuming linear springs and dampers for each contact interface. Inoue and Hirai [9, 17] developed a model for dynamic modeling and orientation control of a rigid object during soft finger grasping and manipulation. To model the softness of fingertips, they assumed a continuous distribution of linear springs positioned perpendicularly to the backplate of the soft fingertip.

Slippage often happens in the contact interface of fingers and objects and control of this slippage is essential for stable and robust grasping and manipulation. However, in the majority of prior studies in this field, it is presumed that the friction coefficients between soft fingers and objects are high enough and slippage never happens during the grasping and manipulation. Hadian et al. [18] studied analysis and control of slippage in object manipulation using a planar rigid-tip finger. Song et al. [19] developed a novel method for prediction and compensation of dynamic slip which occurs between an object and a pair of fingers with hemispherical rigid tips. Engeberg and Meek [20] designed a controller for prosthetic hands to simultaneously prevent slip and minimize the contact force of grasped objects. Kao and Cutkosky [21] modeled the quasi-static sliding manipulation using friction limit surface, however, they did not consider the dynamics of the soft tip. Xu et al. [22] demonstrated a friction model for the contact interface between a soft object and a pair of soft parallel gripper jaws using the Finite Element Method. Ozawa and Tahara [23] investigated past studies on grasping and manipulation of multi-fingered robotic hands from a control viewpoint. Fakhari et al. [24] studied the *linear slippage* which occurs between a *planar soft finger* and an object during manipulation. However, analysis and control of *planar slippage* occurring during manipulating an object using a *spatial soft finger* has not been considered yet.

Therefore, in this paper which is a continuation of our prior work [25], a revised and more general method for dynamic modeling of all different states of planar slippage is presented using the concept of friction limit surface. In this method, different states of planar contact (i.e., stationary, incipient slip, and slippage) are replaced with a second-order differential equation in which its coefficients are determined based on a table. As an example of the proposed method application, object manipulation using a three-link soft finger is studied first. Then, a controller is designed to reduce and remove the undesired slippage occurring between the soft finger and object and simultaneously move the object on a predefined path despite the slippage occurrence.

Slippage analysis in planar contact

Contact forces and moment

Coulomb friction is one of the basic and commonly used dry friction models that determines the tangential frictional force, $\mathbf{f}_t$, between two rigid objects in *point contact* as $|\mathbf{f}_t| \leq \mu N$, where μ is the friction coefficient between two objects and N is the normal force. However, when two objects come into *planar contact* (Fig. 2), the friction cone is replaced with a friction limit surface [2, 3]. Friction limit surface relates contact frictional force/moment to contact sliding motions and determines when there is a planar slippage between the objects. By calculating the contact frictional force and moment for all possible translational and rotational slippage that can occur in the contact interface, the friction limit surface is constructed [3, 25]. In Fig. 3, cross-section view of friction limit surface for a rectangular contact interface when pressure distribution is assumed to be uniform is shown as a sample.

When the contact frictional forces, (i.e., f_x and f_y), and moment, (i.e., m_z), as shown in Fig. 2, are placed inside the friction limit surface boundary, there will be

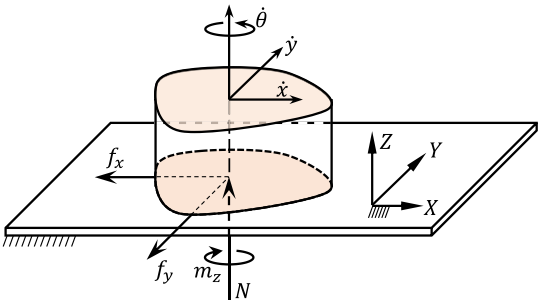

Fig. 2 Contact forces and moment of two objects in planar slippage

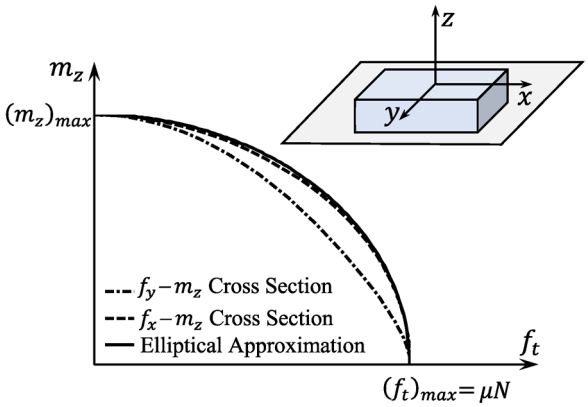

Fig. 3 Cross section view of friction limit surface for a rectangular contact interface

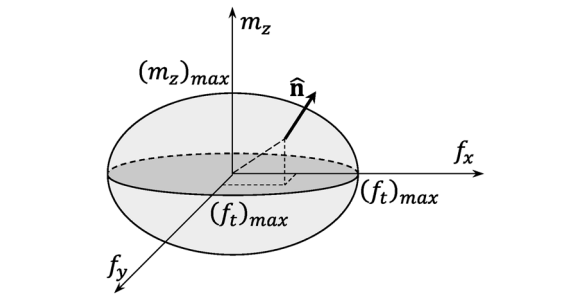

Fig. 4 Ellipsoidal approximation of friction limit surface

no slippage between two objects. By increasing these forces and moment towards the boundary, translational and rotational slippage between two objects begins. This slippage is indeed parallel with the unit vector, $\hat{\mathbf{n}}$, normal to the surface at the point (f_x, f_y, m_z) as shown in Fig. 4. Note that, in pure translational slippage where $m_z = 0$, the locus of the contact frictional forces is a circle in the $f_x - f_y$ plane and its radius is $(f_t)_{\max} = \mu N$.

It is proven that an acceptable approximation for friction limit surface, in general, is an ellipsoid [3]. This ellipsoid fits the maximum frictional force, $(f_t)_{\max}$, and also maximum frictional moment, $(m_z)_{\max}$, as shown in Fig. 4. This simplified model is still relatively accurate and it is proper for dynamic modeling and control of object grasping and manipulation. Moreover, it is shown that the skewness in the pressure distribution at the contact interface of a soft hemispherical fingertip due to tangential forces does not have a significant effect on the shape of the friction limit surface [26]. Therefore, the ellipsoidal approximation of friction limit surface (Fig. 4) can be formulated as

$$\frac{{f_x}^2}{(f_t)^2_{\max}} + \frac{{f_y}^2}{(f_t)^2_{\max}} + \frac{{m_z}^2}{(m_z)^2_{\max}} = 1. \tag{1}$$

Since the planar slippage in the contact interface of two objects is parallel with the unit vector, $\hat{\mathbf{n}}$, normal to the friction limit surface at the point (f_x, f_y, m_z), the relationship between the translational velocities of sliding object along x and y axes, $(\dot{x}, \dot{y})$, angular velocity of sliding object along z axis, $\dot{\theta}$, tangential frictional force, f_t, and frictional moment, m_z, for ellipsoidal approximation of friction limit surface is

$$\frac{\sqrt{\dot{x}^2 + \dot{y}^2}}{\dot{\theta}} = \lambda^2 \frac{f_t}{m_z}, \tag{2}$$

where λ is defined as

$$\lambda = \frac{(m_z)_{\max}}{(f_t)_{\max}}. \tag{3}$$

Slippage modeling of planar contact

Based on the features of ellipsoidal approximation of the friction limit surface (i.e., Eqs. 1 and 2) in the slippage state of a planar contact, the relationship between the contact frictional forces, contact frictional moment, linear sliding velocities, and angular sliding velocity is proposed as

$$\begin{bmatrix} f_x \\ f_y \\ m_z/\lambda \end{bmatrix} = \frac{-\mu N}{\sqrt{\dot{x}^2 + \dot{y}^2 + (\lambda\dot{\theta})^2}} \begin{bmatrix} \dot{x} \\ \dot{y} \\ \lambda\dot{\theta} \end{bmatrix}. \tag{4}$$

Thus, the different states of frictional forces and moment between two objects in planar contact can be represented as

$$\begin{aligned} &{f_x}^2 + {f_y}^2 + \frac{{m_z}^2}{\lambda^2} < (\mu N)^2 && \text{(Stationary)} \\ &{f_x}^2 + {f_y}^2 + \frac{{m_z}^2}{\lambda^2} = (\mu N)^2 && \text{(Incipient Slip)} \\ &\begin{bmatrix} f_x \\ f_y \\ m_z \end{bmatrix} = \frac{-\mu N}{\sqrt{\dot{x}^2 + \dot{y}^2 + (\lambda\dot{\theta})^2}} \begin{bmatrix} \dot{x} \\ \dot{y} \\ \lambda^2\dot{\theta} \end{bmatrix} && \text{(Slippage)} \end{aligned} \tag{5}$$

Since in incipient slip state the object is stationary and the contact frictional forces and moment are placed on the friction limit surface boundary, the second relation of Eq. 5 can also be written as

$$\begin{bmatrix} f_x \\ f_y \\ m_z \end{bmatrix} = \frac{\mu N}{\sqrt{\bar{f}_x^2 + \bar{f}_y^2 + (\bar{m}_z/\lambda)^2}} \begin{bmatrix} \bar{f}_x \\ \bar{f}_y \\ \bar{m}_z \end{bmatrix}, \tag{6}$$

where $\bar{f}_x$, $\bar{f}_y$, and $\bar{m}_z$ are the contact forces and moment when $\dot{\mathbf{X}} = [\dot{x}, \dot{y}, \dot{\theta}]^{\mathrm{T}} = \mathbf{0}$ (i.e., when the contact is assumed to be stationary). Equations 5 and 6 can be combined and rewritten as a single second-order differential equation to model the different states of frictional forces and moment in the planar contact as

$$\beta_1 \ddot{\mathbf{X}} + \begin{bmatrix} \beta_{21}\mathbf{I}_3 & \boldsymbol{\beta}_{22} \end{bmatrix} \mathbf{F} = \mathbf{0}, \tag{7}$$

where $\mathbf{F} = [f_x, f_y, m_z, N]^{\mathrm{T}}$, $\mathbf{I}_3$ is a 3×3 identity matrix, and parameters β_1, β_{21}, and $\boldsymbol{\beta}_{22}$ can be determined using Table 1 based on the different states of the contact.

Manipulating a rigid object using a three-link soft finger

In this section, manipulation of a rigid object on a horizontal surface using a three-link soft finger is studied as an example of application of the method proposed in the previous section. Then, in the next section, a controller is designed to reduce the undesired slippage which occurs during the manipulation of the object. In Fig. 5, top and side views of a soft finger manipulating an object are shown. The soft finger consists of three rigid links and a soft hemisphere attached to the end of the last link to move the object on a horizontal plane. In order to accurately model dynamic equations of the soft finger, dynamics of the soft fingertip is integrated into dynamics of finger linkage.

Table 1 Parameters β_1, β_{21}, and β_{22} in different states of planar contact

	$\dot{\mathbf{X}} \neq \mathbf{0}$	$\dot{\mathbf{X}} = \mathbf{0}$	
	Slippage	**1st Assumption: stationary**	**2nd Assumption: incipient slip**
β_1	0	1	0
β_{21}	1	0	1
$\boldsymbol{\beta}_{22}$	**A**	$\mathbf{0}_{3\times1}$	**C**
Condition to be checked	–	$B < 1$	If 1st Assumption is not correct

$\mathbf{X} = [x, y, \theta]^{\mathrm{T}}$,
$\mathbf{A} = \mu\left(\dot{x}^2 + \dot{y}^2 + \lambda^2\dot{\theta}^2\right)^{-\frac{1}{2}}[\dot{x}, \dot{y}, \lambda^2\dot{\theta}]^{\mathrm{T}}$,
$B = \left(f_x^2 + f_y^2 + m_z^2/\lambda^2\right)/(\mu N)^2$,
$\mathbf{C} = -\mu\left(\bar{f}_x^2 + \bar{f}_y^2 + \bar{m}_z^2/\lambda^2\right)^{-\frac{1}{2}}\left[\bar{f}_x, \bar{f}_y, \bar{m}_z\right]^{\mathrm{T}}$,
where $\bar{f}_x$, $\bar{f}_y$, and $\bar{m}_z$ are calculated from the 1st Assumption

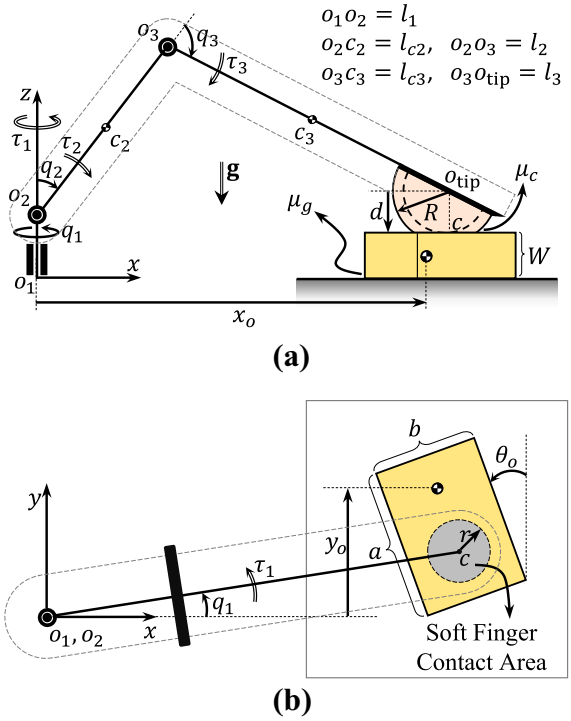

Fig. 5 Object manipulation using a soft finger, **a** side view, **b** top view

Power-law model is one of the time-independent nonlinear elastic contact models that has been proposed for deformation in the contact between a soft hemisphere and a rigid plate as shown in Fig. 6. This model has been theoretically and experimentally validated for different types of soft materials [6, 27] and is presented by

$$r = cN^{\gamma}, \tag{8}$$

where r is the radius of contact area, N is contact normal force, and c and γ are constants which depend on the geometry and material property of the soft fingertip. Due to the accuracy of this model, it is utilized for modeling

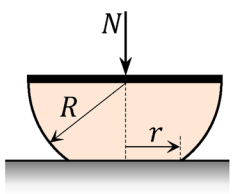

Fig. 6 Contact Interface of a hemispherical soft finger under a normal force

the elastic behavior of the fingertip in this research. Furthermore, as it is also assumed in the previous research [8, 9, 28], the damping behavior of the hemispherical tip is model by a linear viscous damper, i.e., C_{eq} in Fig. 7b.

In order to drive the dynamic equations of the soft finger, Lagrange method is used. Since this system includes both viscous damper and external forces, Lagrange equation can be written as

$$\frac{\mathrm{d}}{\mathrm{d}t}\left(\frac{\partial L}{\partial \dot{q}_i}\right) - \frac{\partial L}{\partial q_i} + \frac{\partial F_{\text{st}}}{\partial \dot{q}_i} = Q_{i,\text{nc}}, \quad i = 1,2,3,4, \tag{9}$$

where

$$\begin{cases} L = T - V : \text{Lagrangian} \\ T : \text{Total Kinetic Energy} \\ V : \text{Total Potential Energy} \\ F_{\text{st}} = C_{\text{eq}}\dot{d}^2/2 : \text{Rayleigh Dissipation Function} \\ Q_{i,\text{nc}} : \text{Generalized Force} \\ q_i : \text{Generalized Coordinate} \end{cases}. \tag{10}$$

Since dynamics of the soft tip is integrated with dynamics of finger linkage, the vector of soft finger generalized coordinates is defined as $\mathbf{q} = [q_1, q_2, q_3, d]^{\mathrm{T}}$, where q_1, q_2, and q_3 are the joint angles and d is the deformation of soft tip (Fig. 5).

We define three *sliding states* x_s, y_s, and θ_s as

$$\begin{aligned} \dot{x}_s &= V_c^x - \dot{x}_o \\ \dot{y}_s &= V_c^y - \dot{y}_o \\ \dot{\theta}_s &= \omega_c^z - \dot{\theta}_o \end{aligned}. \tag{11}$$

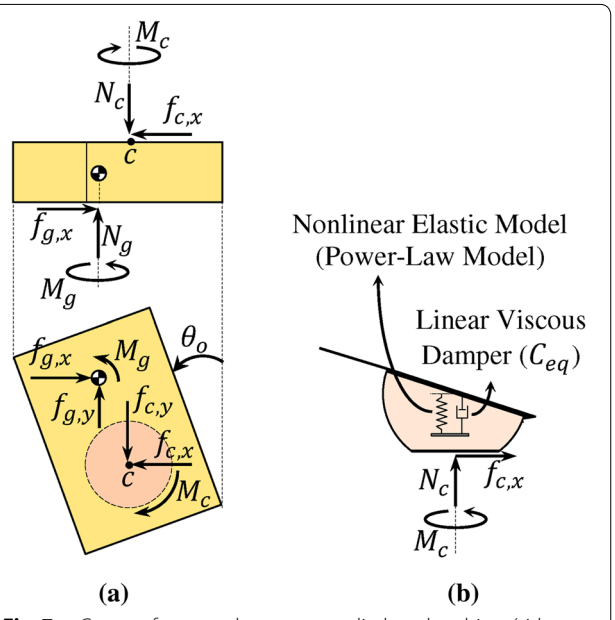

Fig. 7 **a** Contact forces and moment applied on the object (side and top view), **b** soft tip model and the contact forces and moment between the soft finger and the object

In these equations, V_c^x and V_c^y are the linear velocities of point c (Fig. 5), along x and y axes respectively, ω_c^z is the angular velocity of the contact interface about z axis, x_o and y_o represent coordinate of the object center of mass, and θ_o is the rotation of the object (Fig. 5).

Hence, the dynamic equations of the soft finger manipulating a rigid object can be derived as

$$\begin{aligned} &\mathbf{M}(\mathbf{q})\ddot{\mathbf{q}} + \mathbf{h}(\mathbf{q},\dot{\mathbf{q}}) = \mathbf{B}\boldsymbol{\tau} + \mathbf{J}(\mathbf{q})^{\mathrm{T}}\mathbf{F}_c \\ &\mathbf{M}_o\ddot{\mathbf{q}}_o + \mathbf{h}_o = \mathbf{F}_g - \mathbf{B}_c\mathbf{F}_c \\ &\mathbf{J}(\mathbf{q})\ddot{\mathbf{q}} - \mathbf{B}(\ddot{\mathbf{q}}_o + \ddot{\mathbf{q}}_s) = -\dot{\mathbf{J}}(\mathbf{q},\dot{\mathbf{q}})\dot{\mathbf{q}} \\ &\beta_{s,1}\ddot{\mathbf{q}}_s + \mathbf{B}_s(\dot{\mathbf{q}}_s)\mathbf{F}_c = \mathbf{0} \\ &\beta_{o,1}\ddot{\mathbf{q}}_o + \mathbf{B}_o(\dot{\mathbf{q}}_o)\mathbf{F}_g = \mathbf{0} \end{aligned}, \tag{12}$$

where $\mathbf{F}_c = [f_{c,x}, f_{c,y}, M_c, N_c]^{\mathrm{T}}$ represents the contact forces and moment between the soft tip and the object and $\mathbf{F}_g = [f_{g,x}, f_{g,y}, M_g, N_g]^{\mathrm{T}}$ represents the contact forces and moment between the object and the ground as shown in Fig. 7, respectively. Note that the first relation is the soft finger dynamics, the second relation is the object dynamics, the third relation represents the contact constraint and also sliding states (Eq. 11). Two last relations demonstrate the dynamics of frictional forces and moments in the both contact interfaces, i.e., between soft tip and the object and also between the object and ground, derived using the proposed method in the previous section (Eq. 7). In Eq. 12, $\mathbf{M}_4 \times 4$ is the soft finger inertia matrix, $\mathbf{h}_4 \times 1$ is vector of centrifugal, Coriolis, and gravity terms of the soft finger, $\boldsymbol{\tau} = [\tau_1, \tau_2, \tau_3]^{\mathrm{T}}$ is vector of soft finger joint torques (Fig. 5), $\mathbf{B}_4 \times 3$ is a linear mapping between dynamics of the finger linkage (including the soft tip) and the finger joint torques, $\mathbf{B}_{c,4\times4}$ is a matrix used to include moments of the forces $f_{c,x}$ and $f_{c,y}$ about the object center of mass in the object dynamics, $\mathbf{J}_{4\times4}$ is soft finger Jacobian matrix, $\mathbf{M}_{o,4\times3}$ is object inertial matrix, $\mathbf{h}_{o,4\times1}$ is object gravity vector, $\mathbf{q}_o = [x_o, y_o, \theta_o]^{\mathrm{T}}$ is a vector that represents position of the object center of gravity and orientation of the object about its center of gravity, $\mathbf{q}_s = [x_s, y_s, \theta_s]^{\mathrm{T}}$ is vector of sliding states, $\mathbf{B}_s = [\beta_{s,21}\mathbf{I}_3, \boldsymbol{\beta}_{s,22}]$, and $\mathbf{B}_o = [\beta_{o,21}\mathbf{I}_3, \boldsymbol{\beta}_{o,22}]$. The parameters $\beta_{s,1}$, $\beta_{s,21}$, $\boldsymbol{\beta}_{s,22}$, $\beta_{o,1}$, $\beta_{o,21}$, and $\boldsymbol{\beta}_{o,22}$ can be determined using Table 1 based on the different states of each contact and knowing the friction coefficient between soft tip and object, μ_c, and between object and ground, μ_g. Moreover, parameter λ (Eq. 3) which appears in $\boldsymbol{\beta}_{s,22}$ as λ_c for a circular contact interface and in $\boldsymbol{\beta}_{o,22}$ as λ_g for a rectangular contact interface is derived as

$$\begin{aligned} \lambda_c &= \frac{3}{4}\frac{\Gamma(3/k)^2}{\Gamma(2/k)\Gamma(4/k)}r \\ \lambda_g &= \frac{1}{ab}\int_{-b/2}^{b/2}\int_{-a/2}^{a/2}\sqrt{x^2+y^2}\,\mathrm{d}x\mathrm{d}y \end{aligned}, \tag{13}$$

where r is the radius of contact area, $\Gamma(\cdot)$ is the Gamma function, k depends on the shape of the pressure distribution profile in the contact interface of the soft tip [6], and a and b are length and width of the object, respectively. Vector $\mathbf{h}_o$ and matrices $\mathbf{J}(\mathbf{q})$, $\mathbf{M}_o$, $\mathbf{B}$, and $\mathbf{B}_c$ are presented in Appendix.

Slippage control in planar manipulation of the object

Human hands can grasp and manipulate different objects without having knowledge about the weight of objects and the friction coefficient between the fingertips and objects. Indeed, human hands can first sense the incipient slip which occurs in the contact interface of the fingertip by detecting micro-vibrations using the tactile mechanoreceptors and then control the grasp force unconsciously to have a stable grasp and robust manipulation without damaging the objects [29].

In this section, a controller is proposed for the soft finger to move the object on a predefined desired path in a horizontal plane and simultaneously reduce and remove the slippage occurring between the soft fingertip and the object by increasing the normal contact force. The controller is designed based on hybrid position/force control concept and independent of the object parameters, i.e., object mass, m_o, and friction coefficient of object/ground contact, μ_g.

The dynamic equation of the soft finger (i.e., the first relation of Eq. 12) can be rewritten as

$$\begin{aligned} &\mathbf{M}_r\ddot{\mathbf{q}}_r + \mathbf{h}_r = \boldsymbol{\tau} + {\mathbf{J}_c}^{\mathrm{T}}\mathbf{F}_c \\ &N_c = \left(R^2 - d^2\right)^{\frac{1}{2\gamma}} \left(\frac{1}{c}\right)^{\frac{1}{\gamma}} - C_{eq}\dot{d} \end{aligned}, \tag{14}$$

where $\mathbf{M}_r = \mathbf{M}(1{:}3, 1{:}3)$ is inertia matrix of the finger linkage, $\mathbf{h}_r = \mathbf{h}(1{:}3)$ is vector of centrifugal, Coriolis, and gravity terms of the finger linkage, $\mathbf{J}_c = \mathbf{J}(1{:}4, 1{:}3)$ is Jacobian matrix of soft finger contact point c, and $\mathbf{q}_r = [q_1, q_2, q_3]^{\mathrm{T}}$ is the vector of soft finger joint angles. Note that $\mathbf{M}(1{:}3, 1{:}3)$ represents a 3×3 matrix constructed by the first three rows and columns of $\mathbf{M}$, $\mathbf{h}(1{:}3)$ represents a 3×1 vector constructed by the first three components of $\mathbf{h}$, and $\mathbf{J}(1{:}4, 1{:}3)$ represents a 4×3 matrix constructed by the first four rows and the first three columns of $\mathbf{J}$.

The relation between angular velocity of the soft finger joints and velocity of the center of soft finger hemisphere, o_{tip}, with respect to xyz-coordinate system (Fig. 5), can be written by a 3×3 Jacobian matrix, $\mathbf{J}_t$, as

$$\dot{\mathbf{X}}_t = \mathbf{J}_t\dot{\mathbf{q}}_r, \tag{15}$$

where $\mathbf{X}_t = [x_t, y_t, z_t]^{\mathrm{T}}$ is the position of the point o_{tip}. By differentiating Eq. 15, $\ddot{\mathbf{q}}_r$ can be calculated as

$$\ddot{\mathbf{q}}_r = \mathbf{J}_t^{-1}\left(\ddot{\mathbf{X}}_t - \dot{\mathbf{J}}_t\dot{\mathbf{q}}_r\right), \tag{16}$$

and by substituting Eq. 16 into the first relation of Eq. 14, $\boldsymbol{\tau}$ can be derived as

$$\boldsymbol{\tau} = \mathbf{M}_r\mathbf{J}_t^{-1}\left(\ddot{\mathbf{X}}_t - \dot{\mathbf{J}}_t\dot{\mathbf{q}}_r\right) + \mathbf{h}_r - \mathbf{J}_c^{\mathrm{T}}\mathbf{F}_c. \tag{17}$$

The corresponding feedback linearization control for Eq. 17 is given by

$$\boldsymbol{\tau}_c = \mathbf{M}_r\mathbf{J}_t^{-1}\left(\mathbf{a} - \dot{\mathbf{J}}_t\dot{\mathbf{q}}_r\right) + \mathbf{h}_r - \mathbf{J}_c^{\mathrm{T}}\mathbf{F}_c, \tag{18}$$

where $\boldsymbol{\tau}_c$ is the control torques vector of the soft finger joints and $\mathbf{a}$ is the control input vector used to represent the position and force control strategies. By substituting Eq. 18 into Eq. 17, the close-loop equation can be written as

$$\ddot{\mathbf{X}}_t = \mathbf{a}. \tag{19}$$

This equation represents that the task space motion has been globally linearized and decoupled. Since z-axis is always perpendicular to the motion plane of the soft finger contact interface, the position and force controllers can be designed independently. That is, the position controller is designed for the task space variables which represent the tangent motion (i.e., x and y) and the force controller is designed for the task space variable which represents the normal motion (i.e., z). Therefore, vector $\mathbf{a}$ can be written as

$$\mathbf{a} = \begin{bmatrix} \mathbf{a}_T \\ a_N \end{bmatrix}, \tag{20}$$

where

$$\begin{aligned} \mathbf{a}_T &= \ddot{\mathbf{X}}_{t,T}^{\mathrm{des}} + \mathbf{K}_{T,v}\dot{\mathbf{e}}_T + \mathbf{K}_{T,p}\mathbf{e}_T \\ a_N &= \ddot{X}_{t,N}^{\mathrm{des}} + K_{N,v}\dot{e}_N + K_{N,p}e_N \end{aligned}, \tag{21}$$

and $\mathbf{X}_{t,T}^{\mathrm{des}}$ is the object desired trajectory, $\mathbf{K}_{T,v}$ and $\mathbf{K}_{T,p}$ are diagonal positive definite 2×2 matrices, $K_{N,v}$ and $K_{N,p}$ are positive constant parameters, $e_N = X_{t,N}^{\mathrm{des}} - X_{t,N}$, $X_{t,N} = z_t$, and $\dot{X}_{t,N}^{\mathrm{des}} = \ddot{X}_{t,N}^{\mathrm{des}} = 0$. In order to move the object on a desired path even after the slippage between fingertip and object occurs, we define $\mathbf{e}_T$ as $\mathbf{e}_T = \mathbf{X}_{t,T}^{\mathrm{des}} - \mathbf{X}_{o,T}$ where $\mathbf{X}_{o,T} = [x_o, y_o]^{\mathrm{T}}$.

A method for reducing and removing the slippage between the fingertip and object is increasing the normal contact force from an initial value to when the slippage decreases. This method is similar to what human hands do when manipulating an object on a horizontal plane. Hence, the desired normal contact force is proposed as

$$N_c^{\mathrm{des}} = N_c^{\mathrm{ini}} + K_s\Phi(\delta_s, t), \tag{22}$$

where N_c^{ini} is the initial normal contact force, K_s is a constant positive parameter, δ_s is a slippage parameter defined as

$$\delta_s = \left(\dot{x}_s^2 + \dot{y}_s^2 + \lambda_c^2 \dot{\theta}_s^2\right)^{1/2}, \tag{23}$$

and the function $\Phi(\delta_s, t)$ determine the maximum value of δ_s between time 0 and t. Therefore, $X_{t,N}^{\text{des}}$ can be calculated as

$$X_{t,N}^{\text{des}} = z_c + d^{\text{des}}, \tag{24}$$

where z_c is position of center of contact area, c, along z-axis and d^{des} represents the deformation of soft tip when the normal contact force is N_c^{des} and based on Eq. 8, it can be written as

$$d^{\text{des}} = \left(R^2 - c^2\left(N_c^{\text{des}}\right)^{2\gamma}\right)^{1/2}. \tag{25}$$

Numerical simulation and discussion

In this section, performance of the controller designed for manipulating a rigid object on a predefined desired path in the horizontal plane using a three-link soft finger (Fig. 5) is numerically evaluated. In order to solve the dynamic equations of system (i.e., Eq. 12), they can be rewritten in form $\mathbf{b} = \mathbf{A}\mathbf{x}$ as

$$\begin{bmatrix} \mathbf{B}\boldsymbol{\tau} - \mathbf{h} \\ -\mathbf{h}_o \\ -\dot{\mathbf{J}}\dot{\mathbf{q}} \\ \mathbf{0} \\ \mathbf{0} \end{bmatrix} = \begin{bmatrix} \mathbf{M} & \mathbf{0} & \mathbf{0} & -\mathbf{J}^{\mathrm{T}} & \mathbf{0} \\ \mathbf{0} & \mathbf{0} & \mathbf{M}_o & \mathbf{B}_c & -\mathbf{I}_4 \\ \mathbf{J} & -\mathbf{B} & -\mathbf{B} & \mathbf{0} & \mathbf{0} \\ \mathbf{0} & \beta_{s,1}\mathbf{I}_3 & \mathbf{0} & \mathbf{B}_s & \mathbf{0} \\ \mathbf{0} & \mathbf{0} & \beta_{o,1}\mathbf{I}_3 & \mathbf{0} & \mathbf{B}_o \end{bmatrix} \begin{bmatrix} \ddot{\mathbf{q}} \\ \ddot{\mathbf{q}}_s \\ \ddot{\mathbf{q}}_o \\ \mathbf{F}_c \\ \mathbf{F}_g \end{bmatrix}. \tag{26}$$

Block diagram of the closed-loop system is depicted in Fig. 8. In Table 2, the values of the parameters utilized to simulate the system performance are presented. The mass of the soft tip is assumed to be included in the mass of the third link. Note that soft materials generally have a larger friction coefficient compared to rigid materials [30].

The predefined trajectory for the position of the object is assumed to be elliptical as

$$\begin{cases} x^{\text{des}} = A\sqrt{1 - \left(y^{\text{des}}/B\right)^2} \\ y^{\text{des}} = a_0 + a_1 t + a_2 t^2 + a_3 t^3 \end{cases}, \tag{27}$$

where the coefficients are selected as $A = 0.3200$, $B = -0.0905$, $a_0 = -0.0813$, $a_1 = 0$, $a_2 = 0.1219$, and $a_3 = -0.0406$. Moreover, the control parameters are chosen to be $\mathbf{K}_{T,v} = 10\mathbf{I}_2$, $\mathbf{K}_{T,p} = 100\mathbf{I}_2$, $K_{N,v} = 20$, $K_{N,p} = 100$, and $K_s = 20$.

In Fig. 9, the slippage parameter δ_s defined in Eq. 23 and in Fig. 10, the normal force at the contact interface of the soft tip and object are presented. Since the selected initial normal contact force between soft tip and object, i.e., $N_c^{\text{ini}} = 0.05$N, is not sufficient to move the object on the plane, planar slippage begins at the soft tip contact interface. Therefore, the controller increases the normal contact force to reduce the slippage simultaneously. In Fig. 11, the predefined desired

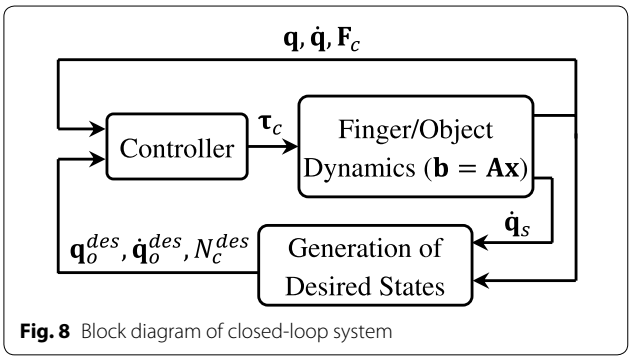

Fig. 8 Block diagram of closed-loop system

Table 2 Simulation parameters

Length (m)		Inertia (kgm^2)		Mass (kg)		Coefficients	
l_1	0.025	$I_{c_1}^{xx}$	$m_1 l_1^2/12$	m_1	0.02	c	0.012
l_2	0.20	$I_{c_1}^{yy}$	$m_1 l_1^2/12$	m_2	0.2	γ	0.02
l_3	0.20	$I_{c_1}^{zz}$	0	m_3	0.2	k	3
l_{c_1}	$l_1/2$	$I_{c_2}^{xx}$	0	m_o	0.1	C_{eq}	300 (Nm/s)
l_{c_2}	$l_2/2$	$I_{c_2}^{yy}$	$m_2 l_2^2/12$			μ_c	0.5
l_{c_3}	$l_3/2$	$I_{c_2}^{zz}$	$m_2 l_2^2/12$			μ_g	0.1
R	0.02	$I_{c_3}^{xx}$	0			λ_c	0.620r (m)
W	0.02	$I_{c_3}^{yy}$	$m_3 l_3^2/12$			λ_g	0.0674 (m)
a	0.20	$I_{c_3}^{zz}$	$m_3 l_3^2/12$				
b	0.15	I_o	$m_o(a^2 + b^2)/12$				

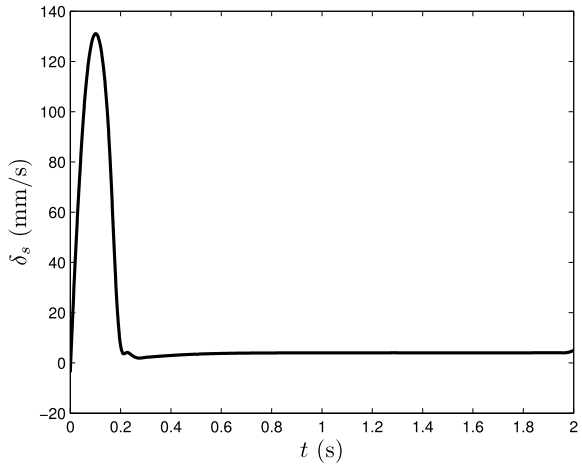

Fig. 9 Slippage parameter

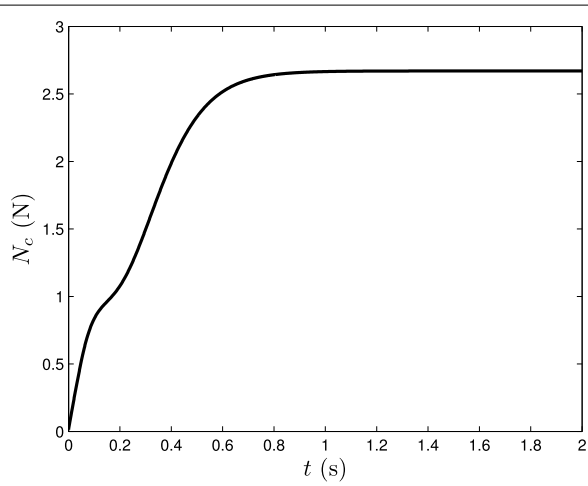

Fig. 10 Normal force at the contact interface of the soft tip and object

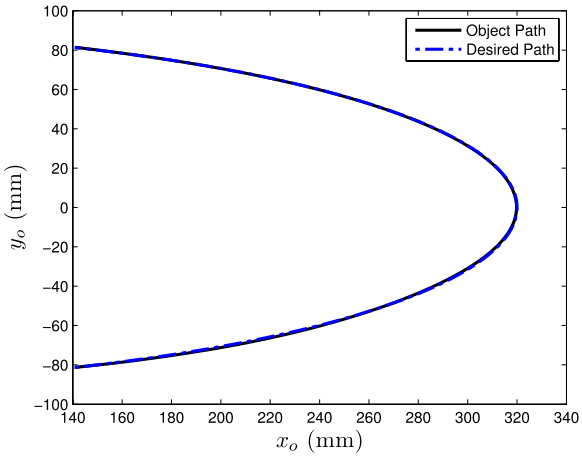

Fig. 11 Comparison of the object path and desired path

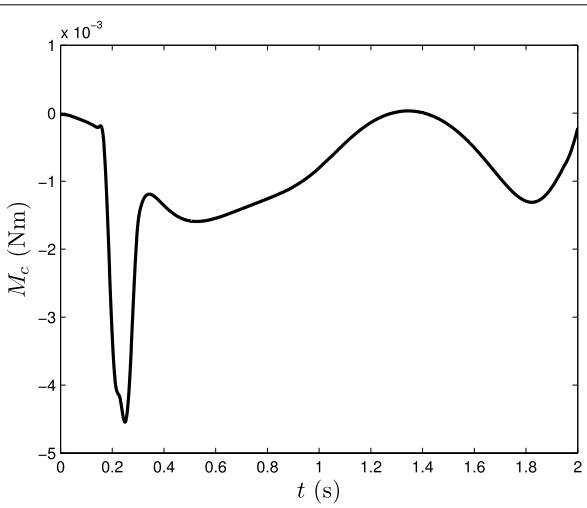

Fig. 12 Frictional moment at the contact interface of the soft tip and object

path and object path are shown. This figure represents that although the slippage occurs at the finger contact interface, the controller is able to move the object on the predefined desired path. In Figs. 12 and 13, the frictional moment and force at the contact interface of soft tip and object are presented (refer to Fig. 7b). Since soft fingers can sustain frictional moment along with tangential frictional force and normal force at the contact interface, they are able to remove the rotational slippage of the object during planar manipulation compared with rigid fingers. Control torques of the finger joints and deformation of the soft tip during manipulation are shown in Figs. 14 and 15.

Uncertainty in friction coefficient

In order to evaluate performance of the controller when the surface condition is changed, we increase the friction coefficient between the object and ground (μ_o) by 100% and 200% in a specific region of the object path (rough surface) as

$$\mu_o = \begin{cases} \mu_{o1} & y_o \leq y_{g1},\ y_o \geq y_{g2} \\ \mu_{o2} & y_{g1} < y_o < y_{g2} \end{cases}, \tag{28}$$

where $\mu_{o1} = 0.1$, $y_{g1} = -0.02$ m, and $y_{g2} = 0.02$ m. Simulation results for $N_c^{ini} = 0.5$ N and three values of μ_{o2}, i.e., 0.1, 0.2, and 0.3, are given in Figs. 16, 17 and 18. As shown in Fig. 16, when the slippage first begins between the finger and object, the controller quickly reduces and cancels the slippage by increasing the normal force

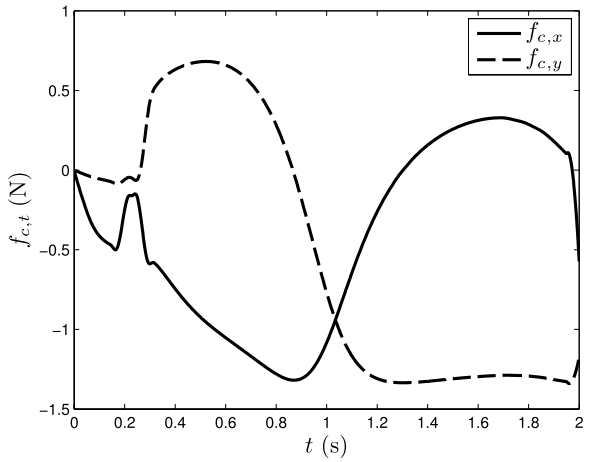

Fig. 13 Tangential frictional forces at the contact interface of the soft tip and object

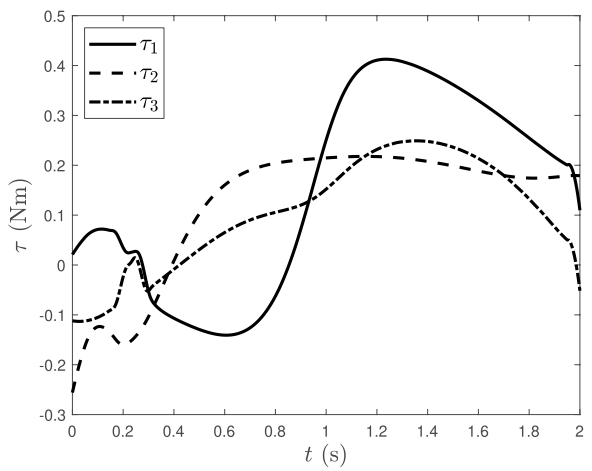

Fig. 14 Control torques of the finger joints

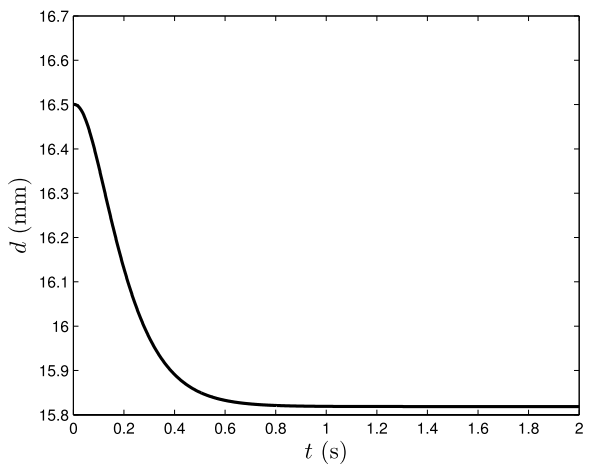

Fig. 15 Deformation of the soft tip during manipulation

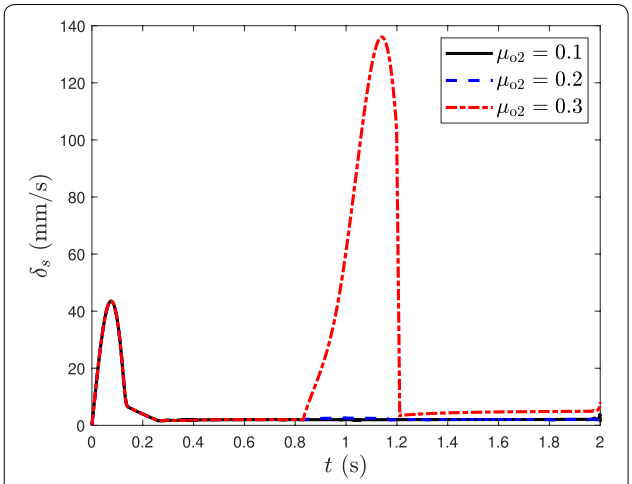

Fig. 16 Slippage parameter

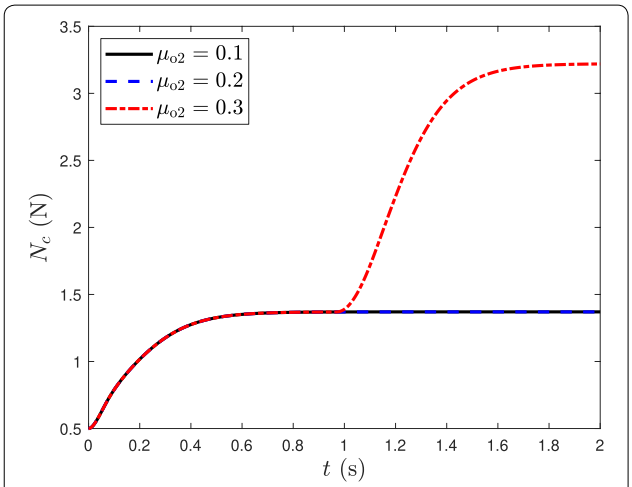

Fig. 17 Normal force at the contact interface of the soft tip and object

(Fig. 17) and moves the object on the predefined desired path. When the object reaches the region with $\mu_{o2} = 0.2$, the slippage between the finger and object does not occur again because the increased normal force is large enough to move the object without slippage. However, when the object reaches the region with a larger friction coefficient, i.e., $\mu_{o2} = 0.3$, the slippage occurs again and the controller increases the normal force to cancel the slippage as much as possible and move the object on the predefined desired path. As shown in Fig. 18, despite reoccurrence of slippage, the object can properly follow the desired path with a deviation less than 4% for when $\mu_{o2} = 0.3$. Hence, the controller has an acceptable performance in moving objects on the surfaces with variable friction coefficients.

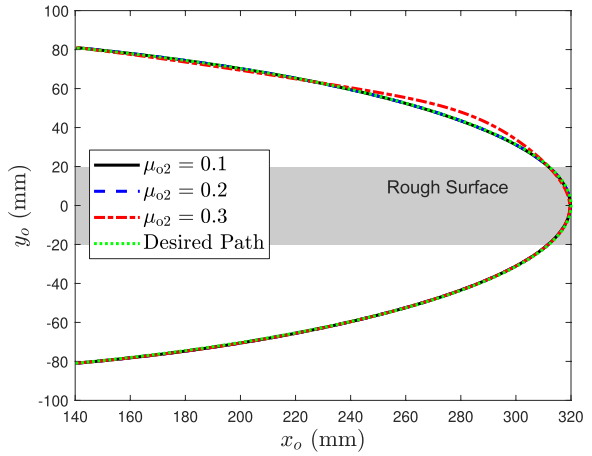

Fig. 18 Comparison of the object path and desired path

Moreover, the performance of the controller has been also evaluated when there is up to 10% uncertainty in the length and mass parameters of the finger and object. The results confirmed the satisfactory robustness of the controller to the parametric uncertainty.

It is worth mentioning that we proposed our dynamic model and controller based on the ellipsoidal approximation of the friction limit surface, which is a generalization of the Coulomb.s friction law. Although this approximation has been validated experimentally [3], due to some other frictional factors, e.g., pre-sliding displacement, stiction effect, Stribeck effect, viscous effect, and frictional lag, this approximation may not be valid for some cases. Hence, in spite of the acceptable performance of the controller in presence of uncertainties, for the situations that the ellipsoidal approximation is not accurate, the controller may have different behavior in the real world from the simulation results and this is a possible limitation of our model.

Conclusions

Contact modeling is one of the first steps in the analysis of grasping and manipulation. When the contact interface is relatively large or deformation in the contact is not negligible, e.g., soft contact, a frictional moment, in addition to tangential frictional force and normal force, can be sustained by the contact interface. Therefore, the friction limit surface is used instead of friction cone to relate contact frictional force/moment to contact sliding motions. In this study, a novel method for dynamic modeling of planar slippage was proposed using the concept of friction limit surface. In this method, a single differential equation was presented to model the different states of frictional force and moment in the planar contact. This method was utilized in the analysis of manipulating a rigid object on a horizontal plane using a three-link soft finger. A controller was designed to reduce and remove the undesired slippage which occurs between the soft finger and object and simultaneously move the object on a predefined path. Numerical simulations revealed that the presented controller has an acceptable performance not only in reducing and removing the undesired finger slippage, but also in moving the object on a predefined desired path despite the slippage occurrence. In the next step, the proposed methods will be utilized for slippage analysis and control in object grasping and manipulation using soft multi-fingered robotic hands.

Acknowledgements
Not applicable.

Authors' contributions
All authors read and approved the final manuscript.

Funding
Not applicable.

Availability of data and materials
Not applicable.

Competing interests
The authors declare that they have no competing interests.

Appendix: Vectors and matrices

The vectors and matrices introduced in Eq. 12 are obtained as

$$\mathbf{J}(\mathbf{q}) = \begin{bmatrix} -s1J_1 & c1J_2 & c1J_3 & 0 \\ c1J_1 & s1J_2 & s1J_3 & 0 \\ 1 & 0 & 0 & 0 \\ 0 & -l_3s23 - l_2s2 & -l_3s23 & -1 \end{bmatrix}, \quad (29)$$
$$J_1 = l_3s23 + l_2s2$$
$$J_2 = l_3c23 + l_2c2 - d$$
$$J_3 = l_3c23 - d$$

$$\mathbf{M}_o = \begin{bmatrix} m_o & 0 & 0 \\ 0 & m_o & 0 \\ 0 & 0 & I_o \\ 0 & 0 & 0 \end{bmatrix}, \qquad \mathbf{h}_o = \begin{bmatrix} 0 \\ 0 \\ 0 \\ m_og \end{bmatrix}, \quad (30)$$

$$\mathbf{B} = \begin{bmatrix} 1 & 0 & 0 \\ 0 & 1 & 0 \\ 0 & 0 & 1 \\ 0 & 0 & 0 \end{bmatrix}, \mathbf{B}_c = \begin{bmatrix} 1 & 0 & 0 & 0 \\ 0 & 1 & 0 & 0 \\ y_o - y_c & x_c - x_o & 1 & 0 \\ 0 & 0 & 0 & 1 \end{bmatrix}, \quad (31)$$

where l_1, l_2, and l_3 are lengths of the finger links (Fig. 5), m_o is the object mass, I_o is moment of inertia of the object about its rotation axis, g is the gravitational acceleration, x_o and y_o represent coordinate of the object center of mass, and x_c and y_c are the position of center of contact

area, c. Furthermore, sI, cI, sIJ, and cIJ represent $\sin(\theta_I)$, $\cos(\theta_I)$, $\sin(\theta_I + \theta_J)$, and $\cos(\theta_I + \theta_J)$, respectively.

Author details
[1] Department of Mechanical Engineering, State University of New York, Korea (SUNY Korea), Incheon 21985, Korea. [2] Department of Mechanical Engineering, Stony Brook University, Stony Brook, NY 11794, USA. [3] Department of Mechanical Engineering, Isfahan University of Technology, 8415683111 Isfahan, Iran.

Received: 26 June 2019 Accepted: 28 October 2019
Published online: 08 November 2019

References

1. Bicchi A (2000) Hands for dexterous manipulation and robust grasping: a difficult road toward simplicity. IEEE Trans Robot Autom 16(6):652–662. https://doi.org/10.1109/70.897777
2. Goyal S, Ruina A, Papadopoulos J (1991) Planar sliding with dry friction: Part 1. limit surface and moment function. Wear 143:307–330
3. Howe R, Cutkosky M (1996) Practical force-motion models for sliding manipulation. Int J Robot Res 15(6):555–572
4. Berselli G, Piccinini M, Palli G, Vassura G (2011) Engineering design of fluid-filled soft covers for robotic contact interfaces: guidelines, nonlinear modeling, and experimental validation. IEEE Trans Robot 27(3):436–449. https://doi.org/10.1109/TRO.2011.2132970
5. Ho VA, Dao DV, Sugiyama S, Hirai S (2011) Development and analysis of a sliding tactile soft fingertip embedded with a microforce/moment sensor. IEEE Trans Robot 27(3):411–424
6. Xydas N, Kao I (1999) Modeling of contact mechanics and friction limit surface for soft fingers in robotics, with experimental results. Int J Robot Res 18(8):941–950
7. Arimoto S, Nguyen PAN, Han HY, Doulgeri Z (2000) Dynamics and control of a set of dual fingers with soft tips. Robotica 18:71–80
8. Kim BH (2004) Motion analysis of soft-fingertip manipulation tasks. Int J Control Autom Syst 2(2):228–237
9. Inoue T, Hirai S (2007) Dynamic stable manipulation via soft-fingered hand. In: IEEE International conference on robotics and automation, pp 586–591. https://doi.org/10.1109/ROBOT.2007.363050
10. Inoue T, Hirai S (2006) Elastic model of deformable fingertip for soft-fingered manipulation. IEEE Trans Robot 22:1273–1279
11. Flugge W (1967) Viscoelasticity. Blaisdell Publishing Company, Waltham
12. Maxwell JC (1867) On the dynamical theory of gases. Philos Trans R Soc Lond 157:49–88. https://doi.org/10.1098/rstl.1867.0004
13. Fung YC (1993) Biomechanics: mechanical properties of living tissues. Springer, Berlin
14. Tiezzi P, Kao I (2006) Characteristics of contact and limit surface for viscoelastic fingers. In: IEEE International conference on robotics and automation, pp 1365–1370
15. Tiezzi P, Kao I (2007) Modeling of viscoelastic contacts and evolution of limit surface for robotic contact interface. IEEE Trans Robot 23(2):206–217
16. Arimoto S, Doulgeri Z, Nguyen P, Fasoulas J (2002) Stable pinching by a pair of robot fingers with soft tips under the effect of gravity. Robotica 20(3):241–249. https://doi.org/10.1017/S0263574701003976
17. Inoue T, Hirai S (2009) Parallel-distributed model in three-dimensional soft-fingered grasping and manipulation. In: IEEE International conference on robotics and automation, pp 2092–2097. https://doi.org/10.1109/ROBOT.2009.5152451
18. Hadian Jazi S, Keshmiri M, Sheikholeslam F, Ghobadi Shahreza M, Keshmiri M (2012) Dynamic analysis and control synthesis of undesired slippage of end-effectors in a cooperative grasping. Adv Robot 26(15):1693–1726. https://doi.org/10.1163/156855308X360776
19. Song X, Liu H, Bimbo J, Althoefer K, Seneviratne LD (2012) A novel dynamic slip prediction and compensation approach based on haptic surface exploration. In: IEEE/RSJ International conference on intelligent robots and systems, pp 4511–4516. https://doi.org/10.1109/IROS.2012.6385897
20. Engeberg ED, Meek SG (2013) Adaptive sliding mode control for prosthetic hands to simultaneously prevent slip and minimize deformation of grasped objects. IEEE/ASME Trans Mechatron 18(1):376–385. https://doi.org/10.1109/TMECH.2011.2179061
21. Kao I, Cutkosky M (1992) Quasistatic manipulation with compliance and sliding. Int J Robot Res 11(1):20–40
22. Xu J, Alt N, Zhang Z, Steinbach E (2017) Grasping posture estimation for a two-finger parallel gripper with soft material jaws using a curved contact area friction model. In: IEEE International conference on robotics and automation, pp 2253–2260. https://doi.org/10.1109/ICRA.2017.7989258
23. Ozawa R, Tahara K (2017) Grasp and dexterous manipulation of multi-fingered robotic hands: a review from a control view point. Adv Robot 31(19–20):1030–1050. https://doi.org/10.1080/01691864.2017.1365011
24. Fakhari A, Keshmiri M, Kao I, Hadian Jazi S (2016) Slippage control in soft finger grasping and manipulation. Adv Robot 30(2):97–108. https://doi.org/10.1080/01691864.2015.1105149
25. Fakhari A, Keshmiri M, Keshmiri M (2014) Dynamic modeling and slippage analysis in object manipulation by soft fingers. In: Proceedings of ASME international mechanical engineering congress and exposition (IMECE), pp 1–10. https://doi.org/10.1115/IMECE2014-38498
26. Fakhari A, Keshmiri M, Kao I (2015) Development of realistic pressure distribution and friction limit surface for soft-finger contact interface of robotic hands. J Intell Robot Syst. https://doi.org/10.1007/s10846-015-0267-2
27. Xydas N, Kao I (2000) Influence of material properties and fingertip size on the power-law equation for soft fingers. In: IEEE/RSJ International conference on intelligent robots and systems, vol 2, pp 1285–1290
28. Shimoga K, Goldenberg A (1996) Soft robotic fingertips part ii: modeling and impedance regulation. Int J Robot Res 15(4):335–350
29. Macefield V, Johansson R (1996) Control of grip force during restraint of an object held between finger and thumb: responses of muscle and joint afferents from the digits. Exp Brain Res 108(1):172–184. https://doi.org/10.1007/BF00242914
30. Cutkosky M, Wright P (1986) Friction, stability and the design of robotic fingers. Int J Robot Res 5(4):20–37

Publisher's Note